MoViC RASD 2016
13th International Conference on Motion and Vibration Control
12th International Conference on Recent Advances in Structural Dynamics
3-6 July 2016, Southampton

Enhanced acoustic transmission into dissipative solid materials through the use of inhomogeneous plane waves

D C Woods, J S Bolton, and J F Rhoads
School of Mechanical Engineering, Ray W. Herrick Laboratories, and Birck Nanotechnology Center, Purdue University, West Lafayette, Indiana, USA

E-mail: jfrhoads@purdue.edu

Abstract. A number of applications, for instance ultrasonic imaging and nondestructive testing, involve the transmission of acoustic energy across fluid–solid interfaces into dissipative solids. However, such transmission is generally hindered by the large impedance mismatch at the interface. In order to address this problem, inhomogeneous plane waves were investigated in this work for the purpose of improving the acoustic energy transmission. To this end, under the assumption of linear hysteretic damping, models for fluid–structure interaction were developed that allow for both homogeneous and inhomogeneous incident waves. For low-loss solids, the results reveal that, at the Rayleigh angle, a unique value of the wave inhomogeneity can be found which minimizes the reflection coefficient, and consequently maximizes the transmission. The results also reveal that with sufficient dissipation levels in the solid material, homogeneous incident waves yield lower reflection values than inhomogeneous waves, due to the large degrees of inhomogeneity inherent in the transmitted waves. Analytical conditions have also been derived which predict the dependence of the optimal incident wave type on the dissipation level and wave speeds in the solid medium. Finally, implications related to the use of acoustic beams of limited spatial extent are discussed.

1. Introduction

Wave propagation in dissipative solid materials is of significant interest in a number of fields, including seismology [1,2], ultrasonic imaging [3], and the nondestructive evaluation of structures [4,5]. In nondestructive testing, for instance, ultrasonic waves can be employed to identify structural defects, and also to indirectly measure material moduli through known relations with measured wave speeds and attenuation coefficients. However, since typical applications require the transmission of ultrasonic waves incident from a fluid medium (e.g., air or water), a substantial portion of the incident energy is reflected at the fluid–solid interface, due to the large differences in impedances between the two media. To address this limitation, incident inhomogeneous plane waves (i.e., waves whose directions of propagation and attenuation are not aligned) are considered here as a pathway to increased energy transmission across real fluid–solid interfaces. Moreover, it is shown that the level ("degree") of inhomogeneity of the incident wave can be tuned, given the dissipation level in viscoelastic media, to optimize the acoustic energy transmission.

Inhomogeneous plane waves can be generated by using phased arrays of sources and the spectral division method [6,7], by propagation of incident homogeneous waves through multilayer

systems [8], or by other approaches [9,10]. Due to material dissipation, both homogeneous and inhomogeneous waves travelling in real media exhibit amplitude attenuation in the direction of phase propagation. Inhomogeneous plane waves also have a component of decay perpendicular to the phase propagation direction, so the angle of amplitude decay relative to the propagation direction, known as the "degree of inhomogeneity" [11], is always less than 90°.

In terms of the material characterization for wave propagation, dissipation is generally modelled as hysteretic damping, as for linear viscoelastic materials [11–13]. With the material further assumed to be homogeneous and isotropic, the phase and attenuation relations, as well as the energy fluxes, of inhomogeneous plane waves (including both longitudinal and shear waves) have been described in detail by Borcherdt [11,14,15] and others [16,17]. The reflection and refraction phenomena of inhomogeneous waves at material interfaces, where linear viscoelastic or fluid media occupy the two semi-infinite half-spaces, have also been described [11,18–22]. Notably, except for the special case of equal dissipation in the two media, the transmitted waves are found to be inhomogeneous even when the incident wave is homogeneous, and transmission is maximized at the Rayleigh angle, where the transmitted longitudinal and shear motions on the solid surface are coincident [11,23,24]. Moreover, the fraction of the incident energy that is transmitted is maximized when the reflection coefficient is minimized.

The goal of the present work was to investigate the use of incident inhomogeneous plane waves to increase the energy transmission across fluid–solid interfaces into dissipative solid media. For the case of lossless media, inhomogeneous incident waves were shown in previous work [25] to yield a zero of the reflection coefficient, and hence optimal energy transmission, which was attained by simultaneously varying the incidence angle and inhomogeneity. Interestingly, for dissipative media and with homogeneous incident waves, Becker and Richardson [26,27] considered arbitrary variation of the shear attenuation coefficient for a water–stainless steel interface, including the variation with frequency, and found that significantly lower values of the reflection coefficient were predicted for certain values of the shear attenuation. In this work, rather than varying the frequency, the degree of inhomogeneity of the incident wave was tuned for the purpose of minimizing the reflection coefficient. The interface model developed here, which allows for both inhomogeneous and homogeneous incident plane waves and arbitrary levels of material dissipation, is based on the theory presented by Borcherdt [11]. Analytical conditions under which inhomogeneous waves improve energy transmission, as compared to homogeneous waves, are derived by using approximations for low-loss media. Numerical results for the reflection coefficient with inhomogeneous incident waves are presented for a low-loss solid interface, and also with the dissipation level varied. Implications related to the construction and use of acoustic beams of limited spatial extent, represented as infinite sums of plane waves, are discussed as well.

2. Representation of inhomogeneous plane waves in dissipative media

When assuming a hysteretic damping model, monochromatic wave propagation in homogeneous, isotropic, linear media may be characterized by the complex material wavenumbers for longitudinal and shear waves, $\tilde{k}_L$ and $\tilde{k}_S$, respectively:

$$\begin{aligned} \tilde{k}_L &= \frac{\omega}{v_L} - j\alpha_L, \\ \tilde{k}_S &= \frac{\omega}{v_S} - j\alpha_S, \end{aligned} \tag{1}$$

where ω is the frequency of the wave, v_L and v_S are the respective wave speeds for homogeneous waves, α_L and α_S are the respective attenuation coefficients, and the time dependence is assumed to be $\exp(j\omega t)$. With a knowledge of the complex wavenumbers and the density ρ, the material

is completely characterized. If the complex Lamé parameters [11] are used as the two material moduli, then the first parameter is given by $\tilde{\lambda} = \rho\omega^2(1/\tilde{k}_P^2 - 2/\tilde{k}_S^2)$, and the second parameter by $\tilde{\mu} = \rho\omega^2/\tilde{k}_S^2$. For the frequency dependence of the wavenumbers, a power law is generally assumed for the attenuation coefficients, which is dependent on the material under consideration, and the variation of the wave speeds is typically much weaker [28].

For homogeneous plane waves, only the frequency, amplitude, and propagation angle with respect to a given coordinate system must be specified to characterize the wave, since the directions of phase propagation and amplitude attenuation are aligned. However, for inhomogeneous plane waves, the degree of inhomogeneity must be additionally specified. Figure 1(a) is a generic diagram of the propagation vector $\vec{P}_i$, attenuation vector $\vec{A}_i$, and degree of inhomogeneity γ_i for an inhomogeneous plane wave propagating in the xz-plane, where, for the sake of generality, the subscript $i = L, S$ indicates the wave type as longitudinal or shear. It follows from the Helmholtz equation that the complex wavevector for either type of wave, $\tilde{\vec{K}}_i = \vec{P}_i - j\vec{A}_i$, must satisfy the material wavenumber condition [11]:

$$\tilde{\vec{K}}_i \cdot \tilde{\vec{K}}_i = \tilde{k}_i^2. \tag{2}$$

In turn, it follows from this relation that when $\alpha_i \neq 0$, the degree of inhomogeneity ($0° \leq \gamma_i < 90°$) is related to the magnitudes of the propagation and attenuation vectors according to:

$$\begin{aligned} |\vec{P}_i|^2 &= \frac{1}{2}\left(\mathrm{Re}[\tilde{k}_i^2] + \sqrt{(\mathrm{Re}[\tilde{k}_i^2])^2 + \frac{(\mathrm{Im}[\tilde{k}_i^2])^2}{\cos^2(\gamma_i)}}\right), \\ |\vec{A}_i|^2 &= \frac{1}{2}\left(-\mathrm{Re}[\tilde{k}_i^2] + \sqrt{(\mathrm{Re}[\tilde{k}_i^2])^2 + \frac{(\mathrm{Im}[\tilde{k}_i^2])^2}{\cos^2(\gamma_i)}}\right), \end{aligned} \tag{3}$$

where Re denotes the real part of the argument and Im the imaginary part. It should be emphasized here that the degree of inhomogeneity, if nonzero, impacts both the effective phase speed $\omega/|\vec{P}_i|$, which is lower than that for homogeneous waves v_i, and the effective attenuation $|\vec{A}_i|$, which exceeds that for homogeneous waves α_i.

Finally, the wave potentials also follow from the solution to the Helmholtz equation which, for longitudinal and shear waves, respectively, are given by [11]:

$$\begin{aligned} \tilde{\phi}_L &= \tilde{\Phi}_L \exp[-\vec{A}_L \cdot \vec{r}] \exp[j(\omega t - \vec{P}_L \cdot \vec{r})], \\ \tilde{\vec{\phi}}_S &= \tilde{\vec{\Phi}}_S \exp[-\vec{A}_S \cdot \vec{r}] \exp[j(\omega t - \vec{P}_S \cdot \vec{r})], \end{aligned} \tag{4}$$

where $\vec{r}$ is the position vector, and $\tilde{\Phi}_L$ and $\tilde{\vec{\Phi}}_S$ are the amplitudes of the potentials.

3. Fluid-solid interface

The reflection and transmission coefficients, as well as the stresses and energy fluxes, are developed here for a semi-infinite material interface between fluid and solid media. Both media are assumed to be homogeneous, isotropic, and linear, and to have an associated hysteretic damping model. The incident wave is taken to be a longitudinal plane wave in the fluid, which may be either homogeneous or inhomogeneous. The interface is shown conceptually in Figure 1(b), where a right-handed, rectangular coordinate system is assumed. For the sake of simplicity, to denote whether quantities apply in the fluid or solid medium, no superscript will be used for the fluid medium, and a superscript prime will be used for the solid (e.g., $\tilde{k}_L$ will denote the material wavenumber for longitudinal waves in the fluid, and $\tilde{k}'_L$ will denote that in the solid).

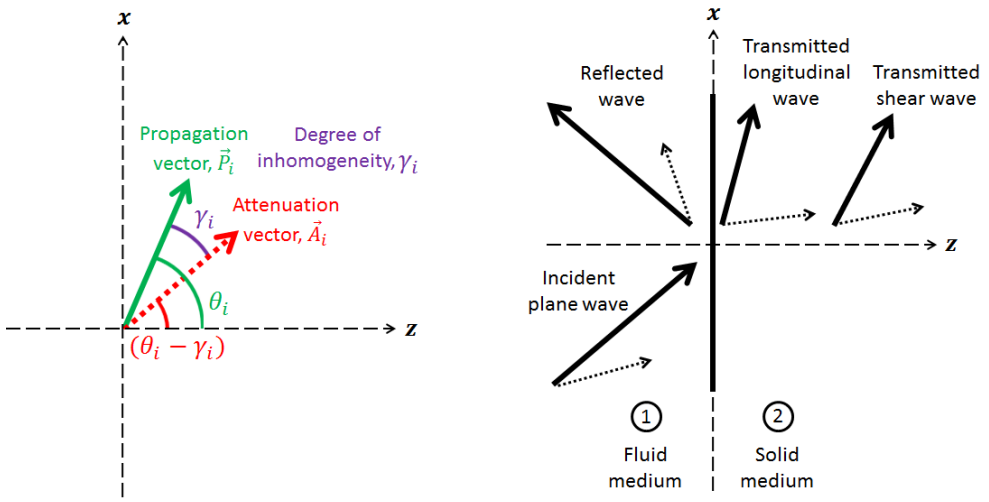

(a) (b)

Figure 1. A diagram showing (a) the propagation and attenuation vectors for an inhomogeneous plane wave propagating in the xz-plane (where the subscript $i = L, S$ indicates the wave type as longitudinal or shear), and (b) the reflected and transmitted waves at the fluid–solid interface for an incident inhomogeneous plane wave. Propagation vectors are shown as solid lines, and attenuation vectors as dotted lines.

The boundary conditions at the interface (i.e., at $z = 0$) require continuity of the stress and particle displacement normal to the interface, and also continuity of the shear stress [11,29]. It is straightforward to compute the particle displacement in either medium from the wave potentials: $\tilde{\vec{u}}^{(m)} = \nabla\tilde{\phi}_L^{(m)} + \nabla \times \tilde{\vec{\phi}}_S^{(m)}$, where the superscript m indicates the medium. For propagation in the xz-plane and with the shear stress in-plane, the normal and shear stresses, respectively, can be computed in either medium as:

$$\begin{aligned} \tilde{\sigma}_{zz}^{(m)} &= \tilde{\lambda}^{(m)} \left(\frac{\partial \tilde{u}_x^{(m)}}{\partial x} + \frac{\partial \tilde{u}_z^{(m)}}{\partial z} \right) + 2\tilde{\mu}^{(m)} \left(\frac{\partial \tilde{u}_z^{(m)}}{\partial z} \right), \\ \tilde{\sigma}_{xz}^{(m)} &= \tilde{\mu}^{(m)} \left(\frac{\partial \tilde{u}_x^{(m)}}{\partial z} + \frac{\partial \tilde{u}_z^{(m)}}{\partial x} \right), \end{aligned} \tag{5}$$

where the subscript on the right-hand-side denotes the component of the displacement vector. It is assumed here that the fluid medium does not sustain shear waves (i.e., $\tilde{\mu} = 0$, $\tilde{\vec{\phi}}_S = 0$), so the displacement and stress equations simplify considerably in the fluid. As a consequence of shear stress continuity, the shear stress at the surface of the solid is thus equal to zero in this case.

The reflection and transmission coefficients are computed by application of the aforementioned boundary conditions. Trace wavenumber continuity, or the generalized Snell's law, subsequently follows: $\tilde{k}_{L,x} = \tilde{k}'_{L,x} = \tilde{k}'_{S,x}$, where the second subscript denotes the component of the wavevector. Therefore, $\tilde{k}_x$ can be simply written without ambiguity. The z-components of the transmitted wavevectors are then computed from the material wavenumber condition, Eq. (2), by using the principal value of the square root [11]: $\tilde{k}'_{L,z} = (\tilde{k}'^2_L - \tilde{k}^2_x)^{1/2}$ and $\tilde{k}'_{S,z} = (\tilde{k}'^2_S - \tilde{k}^2_x)^{1/2}$. Finally, the three boundary conditions yield the linear system that is

solved for the reflection and transmission coefficients:

$$\begin{bmatrix} \tilde{k}_{L,z} & \tilde{k}'_{L,z} & \tilde{k}_x \\ -\tilde{\lambda}\tilde{k}_L^2 & \tilde{\lambda}'\tilde{k}_L'^2 + 2\tilde{\mu}'\tilde{k}_{L,z}'^2 & 2\tilde{\mu}'\tilde{k}_x\tilde{k}'_{S,z} \\ 0 & 2\tilde{\mu}'\tilde{k}_x\tilde{k}'_{L,z} & \tilde{\mu}'(\tilde{k}_x^2 - \tilde{k}_{S,z}'^2) \end{bmatrix} \begin{bmatrix} \tilde{R} \\ \tilde{T}_L \\ \tilde{T}_S \end{bmatrix} = \begin{bmatrix} \tilde{k}_{L,z} \\ \tilde{\lambda}\tilde{k}_L^2 \\ 0 \end{bmatrix}, \tag{6}$$

where $\tilde{R}$ is the (longitudinal) reflection coefficient, and $\tilde{T}_L$ and $\tilde{T}_S$ are the transmission coefficients for the transmitted longitudinal and shear waves, respectively, in terms of the wave potentials.

It is then straightforward to compute the stresses in either medium by using Eq. (5). The instantaneous energy flux vector [11,14,30] is given in terms of the stress tensor $\tilde{\sigma}_{ln}^{(m)}$ and particle velocity vector $\partial\tilde{\vec{u}}^{(m)}/\partial t$:

$$E_n(t) = -\left(\mathrm{Re}\left[\tilde{\sigma}_{xn}^{(m)}\right] \mathrm{Re}\left[\frac{\partial \tilde{u}_x^{(m)}}{\partial t}\right] + \mathrm{Re}\left[\tilde{\sigma}_{zn}^{(m)}\right] \mathrm{Re}\left[\frac{\partial \tilde{u}_z^{(m)}}{\partial t}\right] \right), \tag{7}$$

for $n = x, z$. The average energy flux, or intensity, is then computed by time-averaging the instantaneous flux over one period.

3.1. Minimization of the reflection coefficient

In order to maximize the energy transmitted across the fluid–solid interface, the reflection coefficient should be minimized. Provided that the density and Rayleigh wave speed in the solid exceed the density and longitudinal wave speed, respectively, in the fluid, it is well-known that transmission is optimized when incidence is at the Rayleigh angle for the interface, at which point the incident wave is coincident with the free wave solution of resonant longitudinal and shear motions on the solid surface [23,24,31]. The degree of inhomogeneity of the incident wave also affects the energy transmission, and the optimal value of the inhomogeneity depends on the dissipation levels in the solid, as well as on the other parameters which characterize the interface.

The wavenumber $\tilde{k}'_{Ray}$ for the Rayleigh-type surface wave on a linear viscoelastic half-space can be numerically computed as for a lossless elastic half-space, but with the complex values for the longitudinal and shear material wavenumbers inserted into the characteristic equation [11]:

$$\left(\frac{\tilde{k}_S'^2}{\tilde{k}_{Ray}'^2}\right)^3 - 8\left(\frac{\tilde{k}_S'^2}{\tilde{k}_{Ray}'^2}\right)^2 + \left(24 - 16\frac{\tilde{k}_L'^2}{\tilde{k}_S'^2}\right)\left(\frac{\tilde{k}_S'^2}{\tilde{k}_{Ray}'^2}\right) - 16\left(1 - \frac{\tilde{k}_L'^2}{\tilde{k}_S'^2}\right) = 0, \tag{8}$$

where the solution is the root such that $|\tilde{k}_S'^2/\tilde{k}_{Ray}'^2| < 1$. The complex wave speed $\tilde{v}'_{Ray}$ of the Rayleigh-type wave is then $\tilde{v}'_{Ray} = \omega/\tilde{k}'_{Ray}$, and the Rayleigh angle for the fluid–solid interface is $\theta_{Ray} = \arcsin(v_L/\mathrm{Re}[\tilde{v}'_{Ray}])$, where v_L (unprimed) is the wave speed for homogeneous longitudinal waves in the fluid medium. For low-loss solids, the effect of material dissipation on the Rayleigh wave speed is negligible, and the wave speed can be approximated as: $\tilde{v}'_{Ray} \approx \mathrm{Re}[\tilde{v}'_{Ray}] \equiv v'_{Ray}$.

With respect to the degree of inhomogeneity γ_L of the incident wave which minimizes the reflection coefficient, analysis reveals a strong dependence on the dissipation levels in the solid medium. For the lossless fluid–solid interface, it was shown that, with incidence at the Rayleigh angle, a unique value of the inhomogeneity yields a zero of the reflection coefficient magnitude [25]. For the dissipative fluid–solid interface under consideration here, a unique value for the degree of inhomogeneity can likewise be found which yields a local minimum of the reflection coefficient if the dissipation levels in the solid are sufficiently small. The value of the reflection

coefficient magnitude there is typically near-zero, but remains nonzero due to the material dissipation in the system.

However, above a critical level of dissipation in the solid, homogeneous incident waves yield lower values of the reflection coefficient at the Rayleigh angle than do inhomogeneous incident waves, regardless of the value of the degree of inhomogeneity. This is due to the fact that, with sufficient dissipation levels in the solid, the transmitted waves inherently have a high degree of inhomogeneity, even for homogeneous incident waves, and so there is no benefit to introducing an additional level of inhomogeneity through an inhomogeneous incident wave. Therefore, the reflection coefficient is minimized for a homogeneous incident wave, but the value is neither a local minimum nor typically near-zero (see also Section 4.2).

An approximation for the critical value of solid dissipation below which inhomogeneous incident waves improve energy transmission can be derived by assuming small losses in the solid and negligible losses in the fluid. The derivation is given in the Appendix. The ratio of the longitudinal attenuation coefficient in the solid to the shear attenuation coefficient was held constant in the variation: $\alpha'_{ratio} = \alpha'_L/\alpha'_S = \text{constant}$. The result for the approximation, in terms of the shear attenuation coefficient, is:

$$\alpha'^{*}_S \approx \frac{1}{4}\left(\frac{\rho v_L}{\rho' v'_S}\right)\left(\frac{v'_{Ray}}{\sqrt{v'^2_{Ray} - v^2_L}}\right)\frac{\omega}{V}, \tag{9}$$

where the quantity V is a function of only the wave speeds and attenuation ratio in the solid and is given by Eq. (A.5). The first term in parentheses is the ratio of the longitudinal wave impedance in the fluid to the shear wave impedance in the solid, and the second term accounts for the effect of the incident medium (fluid) on the transmitted waves when incidence is at the Rayleigh angle. If a power law is assumed for the frequency variation of the attenuation coefficient, $\alpha'_S = a\omega^b$, then the condition can instead be framed in terms of the frequency:

$$\omega^* \approx \left[\frac{1}{4aV}\left(\frac{\rho v_L}{\rho' v'_S}\right)\left(\frac{v'_{Ray}}{\sqrt{v'^2_{Ray} - v^2_L}}\right)\right]^{1/(b-1)}. \tag{10}$$

Thus, for a homogeneous incident wave and set material parameters (except for the frequency dependence of the attenuation), a frequency can be found which yields a minimum of the reflection coefficient, a conclusion which is supported by the investigations of Becker and Richardson [26,27]. However, since the present work is focused on the extension to inhomogeneous incident waves, the frequency will be held constant.

4. Numerical results and discussion

For the purpose of illustrating the effect of the degree of inhomogeneity of the incident plane wave on the reflection coefficient, a water–stainless steel interface is considered here, with the incidence angle near the Rayleigh angle for the interface. Additionally, simultaneous variation of the inhomogeneity of the incident wave and the solid dissipation level is considered, and the exact results for the critical value of dissipation are directly compared with those predicted by the approximation in Eq. (9).

4.1. Low-loss solid interface: Water–stainless steel

For a water–stainless steel interface at a frequency of 10 MHz, the material properties were taken as those used by Borcherdt [11]: for water, $\rho = 1000$ kg/m^3, $v_L = 1490$ m/s, and $\alpha_L = 2.530$ rad/m; and for stainless steel, $\rho' = 7932$ kg/m^3, $v'_L = 5740$ m/s, $v'_S = 3142$ m/s, $\alpha'_L = 39.95$

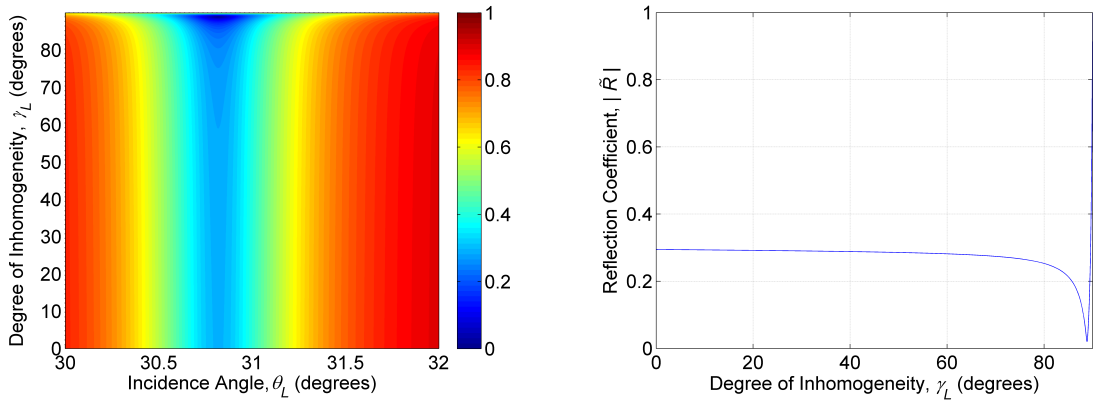

(a) (b)

Figure 2. The magnitude of the reflection coefficient for the water–stainless steel interface at 10 MHz as a function of (a) incidence angle θ_L and degree of inhomogeneity γ_L of the incident wave, and (b) degree of inhomogeneity γ_L of the incident wave at the Rayleigh angle $\theta_L = \theta_{Ray} \approx 30.83°$.

rad/m, and $\alpha'_S = 127.0$ rad/m. The Rayleigh wave speed, from the equations presented in Section 3.1, is $v'_{Ray} \approx 2907$ m/s (where the imaginary part is negligible), and the Rayleigh angle is $\theta_{Ray} \approx 30.83°$.

Figure 2(a) shows the magnitude of the reflection coefficient as the incidence angle θ_L is varied near the Rayleigh angle and the degree of inhomogeneity γ_L is varied from 0° (homogeneous wave) to values near 90°. As is evident, with respect to the variation of the incidence angle, the lowest values of the reflection coefficient are achieved at the Rayleigh angle. More importantly, with incidence at the Rayleigh angle, the variation of the degree of inhomogeneity is observed to yield near-zero reflection values, and hence near-perfect energy transmission into the solid. The degree of inhomogeneity which yields the local minimum is $\gamma_L \approx 88.85°$. This phenomenon is illustrated in Figure 2(b), where only the degree of inhomogeneity is varied, and the incidence angle is held constant at the Rayleigh angle. The value of the reflection coefficient at the local minimum is $|\tilde{R}| \approx 0.0203$, which represents a significant reduction from the value of $|\tilde{R}| \approx 0.295$ for homogeneous incident waves.

4.2. Variation of the solid dissipation level and incident wave inhomogeneity

Though a unique value of the degree of inhomogeneity of the incident wave can be found for low-loss solid interfaces that yields a local minimum of the reflection coefficient at the Rayleigh angle, no such value can be found if dissipation levels in the solid are above a critical level. Since the transmitted waves in such higher-loss solids inherently have considerable degrees of inhomogeneity when incidence is at the Rayleigh angle, no additional benefit is conferred by making the incident wave inhomogeneous. In order to illustrate this effect, the properties of the interface considered in Section 4.1 were used, except that the attenuation coefficients in the solid were varied along with the incident wave inhomogeneity. The ratio of the longitudinal to shear attenuation coefficients in the solid was held constant at the value computed from the parameters in Section 4.1: $\alpha'_{ratio} = \alpha'_L/\alpha'_S = 0.3146$. The frequency was held constant at 10 MHz, and so the variation of the attenuation here is considered to be a simple variation of material parameters, rather than that from frequency dependence.

Figure 3 presents the results for the reflection coefficient magnitude for simultaneous variation of the incident wave inhomogeneity γ_L and solid dissipation level, as specified in terms of the

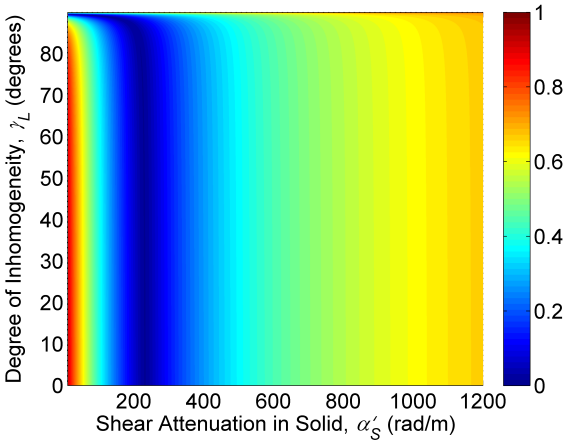

Figure 3. The magnitude of the reflection coefficient at 10 MHz, where the properties are those for the water–stainless steel interface except that the attenuation in steel is varied as shown, as a function of the shear attenuation coefficient in steel α'_S and the degree of inhomogeneity γ_L of the incident wave. The incident wave is propagating at the Rayleigh angle and the ratio of the longitudinal to shear attenuation coefficients in steel is held constant at $\alpha'_{ratio} = 0.3146$.

shear attenuation coefficient α'_S. As can be observed, on the left side of the figure (i.e., at lower losses), there is a locus of small reflection values where, for each value of the attenuation, a unique, nonzero value of the inhomogeneity can be found to yield the minimum of the reflection coefficient. However, above a critical level of dissipation, no such local minima exist and there is simply a slight variation of the reflection coefficient with respect to the incident wave inhomogeneity, where the lowest values occur for homogeneous incident waves (i.e., at $\gamma_L = 0°$).

Based on the variation along the line $\gamma_L = 0°$ in Figure 3, it is clear that the critical value of the attenuation coincides with the local minimum in the reflection coefficient with respect to attenuation for a homogeneous incident wave, which was used in the derivation of the approximation for the critical value, Eq. (9). As such, for a homogeneous incident wave at the Rayleigh angle, Figure 4 presents a direct comparison between the exact result for the reflection coefficient, computed by solving the system in Eq. (6), and the result computed by solving the approximate system derived in the Appendix, as the shear attenuation coefficient is varied. For both the magnitude shown in Figure 4(a) and the phase shown in Figure 4(b), for low values of the attenuation, the approximation is very close to the exact result, as anticipated based on the assumptions used in the approximation. The results diverge, but remain relatively close, as the attenuation is increased towards the critical value, at which point the magnitude is a minimum and the phase passes through $-90°$. With further increases in the attenuation values, the approximation diverges since the low-loss assumptions are violated. The prediction for the critical value based on the approximation, Eq. (9), is $\alpha'^{*}_S \approx 217.9$ rad/m, which yields an error of 6.2% compared to the exact value of $\alpha'^{*}_S = 232.2$ rad/m. In the context of applications which seek to maximize the energy transmitted into the solid, the critical value of the dissipation provides an upper bound below which inhomogeneous incident waves may improve the transmission.

5. Conclusions

A model for the transmission of inhomogeneous plane waves across dissipative fluid–solid interfaces has been presented, where a linear hysteretic damping model was assumed. For low-loss solids, inhomogeneous incident waves were shown to substantially reduce the magnitude of the reflection coefficient in comparison with homogeneous waves, and thus increase the energy

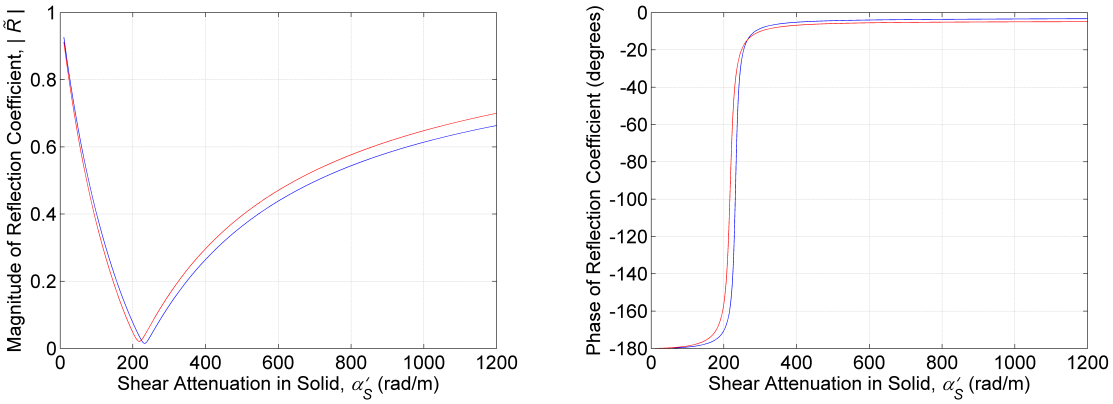

(a) (b)

Figure 4. The (a) magnitude and (b) phase of the reflection coefficient at 10 MHz, where the properties are those for the water–stainless steel interface except that the attenuation in steel is varied as shown, as a function of the shear attenuation coefficient in steel α'_S. The incident wave is homogeneous and is propagating at the Rayleigh angle, and the ratio of the longitudinal to shear attenuation coefficients in steel is held constant at $\alpha'_{ratio} = 0.3146$. The blue curve corresponds to the exact solution, as computed from Eq. (6), and the red curve corresponds to the approximation, as derived in the Appendix.

transmission, for incidence at the Rayleigh angle. Moreover, a unique value of the degree of inhomogeneity could be found which yields the local minimum of the reflection coefficient and, therefore, the maximum energy transmission into the solid at a given frequency. However, above a critical level of material dissipation in the solid, inhomogeneous incident waves were found to yield slightly higher reflection values than homogeneous waves, which is attributable to the high degrees of inhomogeneity inherent in the transmitted waves in higher-loss solids. An analytical approximation was derived for the critical dissipation value, and it was found to give predictions close to the exact result.

Since the inhomogeneity of the incident wave can be controlled by sound field reproduction techniques [6,7,9,10], the use of inhomogeneous plane waves may help to address the transmission limitations in applications such as ultrasonic imaging [3] and nondestructive testing [4,5]. More broadly, this work may inform the construction of acoustic beam profiles of limited spatial extent [23,24,32,33], which are typically used in practice, to optimize the energy transmission across material interfaces. Since bounded acoustic waves, such as Gaussian beams, can be described by a decomposition consisting of an infinite sum of inhomogeneous plane waves [34,35], the reflection and transmission coefficients can be computed for each component, and the reflected and transmitted profiles may subsequently be calculated by summation. Thus, in applications in which it is sought to maximize the energy transmission, the results for inhomogeneous plane waves described in this work may be useful in constructing the components, or "building blocks", for optimal wave profiles for a given interface.

Future work will extend the present work to incident waves of finite extent by analyzing common wave profiles and by constructing new profiles from optimal plane wave components. Sound field reproduction techniques will also be further considered for the purpose of constructing arbitrary wave profiles and inhomogeneous plane wave approximations. That work will continue the investigation of methods for increased acoustic energy transmission across fluid–solid interfaces through theory and experimentation.

Acknowledgements
This research is supported by the U.S. Office of Naval Research by way of a Multidisciplinary University Research Initiative on Sound and Electromagnetic Interacting Waves under ONR Grant No. N00014-10-1-0958.

Appendix: Derivation of the critical value of solid dissipation below which inhomogeneous waves minimize reflection

An approximation for the critical value of the shear attenuation coefficient below which inhomogeneous incident plane waves improve the energy transmission at the Rayleigh angle is derived here. Since the degree of inhomogeneity of the incident wave which minimizes the reflection coefficient magnitude is zero in the right-hand limit at the critical value of attenuation (see also Section 4.2), the system in Eq. (6) can be analyzed to minimize $\tilde{R}$ for a homogeneous incident wave.

In order to simplify the system, the losses in the fluid are assumed to be negligible compared to the real part of the incident wavevector and compared to the losses in the solid: $\alpha_L \ll \omega/v'_{Ray}$ and $\alpha_L \ll \alpha'_L, \alpha'_S$. These conditions yield, for the fluid:

$$\tilde{\lambda} \approx \rho v_L^2, \quad \tilde{k}_x \approx \frac{\omega}{v'_{Ray}}, \quad \tilde{k}_{L,z} \approx \frac{\omega\sqrt{v'^2_{Ray} - v_L^2}}{v'_{Ray} v_L}. \tag{A.1}$$

In the solid, the losses are assumed to be small in the sense that the squares of the attenuation coefficients are negligible in comparison to those of the real parts of the material wavenumbers: $\alpha'^2_L, \alpha'^2_S \ll (\omega/v'_L)^2, (\omega/v'_S)^2$. Thus, the imaginary part of the complex Rayleigh-type wave speed can be neglected and the real part v'_{Ray} is sufficient. The imaginary part of the first Lamé parameter is also neglected here for the purpose of stress computations, since the effects of the longitudinal and shear attenuation coefficients partially offset each other for the first Lamé parameter. Consequently, for the solid:

$$\tilde{\lambda'} \approx \rho' \left(v'^2_L - 2v'^2_S\right), \quad \tilde{\mu'} \approx \rho' v'^2_S \left(1 + \frac{2jv'_S\alpha'_S}{\omega}\right). \tag{A.2}$$

The z-components of the transmitted wavevectors are computed by using the principal value of the square root, and must also be approximated here. This approximation can be made by using the assumptions listed above, the material wavenumber condition in Eq. (2), and the observation that the magnitudes of the real part of the z-components are small for supercritical incidence at the Rayleigh angle (i.e., $|\mathrm{Re}[\tilde{k}'_{L,z}]| \ll |\mathrm{Im}[\tilde{k}'_{L,z}]|$ and $|\mathrm{Re}[\tilde{k}'_{S,z}]| \ll |\mathrm{Im}[\tilde{k}'_{S,z}]|$). The real and imaginary parts of the resulting equation then yield the approximations for the real and imaginary parts of the z-components of the transmitted wavevectors:

$$\begin{aligned}
\tilde{k}'_{L,z} &\approx \frac{\alpha'_L}{v'_L\sqrt{v'^{-2}_{Ray} - v'^{-2}_L}} - j\omega\sqrt{v'^{-2}_{Ray} - v'^{-2}_L}, \\
\tilde{k}'_{S,z} &\approx \frac{\alpha'_S}{v'_S\sqrt{v'^{-2}_{Ray} - v'^{-2}_S}} - j\omega\sqrt{v'^{-2}_{Ray} - v'^{-2}_S}.
\end{aligned} \tag{A.3}$$

The substitution of the above approximations into Eq. (6) yields an approximation to the system in terms of only the frequency ω and the material parameters sufficient to characterize the two media under the assumptions used (ρ, ρ', v_L, v'_L, v'_S, α'_L, α'_S, and, as computed from the relations highlighted in Section 3.1, v'_{Ray}). Finally, the ratio of the longitudinal attenuation

coefficient in the solid to the shear attenuation coefficient is held constant in the variation: $\alpha'_{ratio} = \alpha'_L/\alpha'_S =$ constant. The system can then be solved by row reduction and, given the assumptions used here, terms of order $(\alpha'_S)^2$ and higher can be neglected.

The minimum of the reflection coefficient magnitude with respect to the attenuation occurs when the real part of the reflection coefficient is zero. Thus, setting that part equal to zero yields the approximation for the critical value of the shear attenuation coefficient:

$$\alpha'^{*}_S \approx \frac{1}{4}\left(\frac{\rho v_L}{\rho' v'_S}\right)\left(\frac{v'_{Ray}}{\sqrt{v'^2_{Ray} - v^2_L}}\right)\frac{\omega}{V}, \tag{A.4}$$

where the quantity V (with units of velocity) is a function of only the wave speeds and attenuation ratio in the solid and is given by:

$$\begin{aligned} V(v'_L, v'_S, v'_{Ray}, \alpha'_{ratio}) = \xi_S &\left[v'^2_S v'^{-2}_{Ray}(1 + 2v'^2_S \xi_S^{-2})\right] \\ &- \xi_L \left[v'^2_S \xi_L^{-2} + v'^{-2}_L (v'^2_S - v'^2_L/2) + v'^3_S (v'^{-2}_{Ray} + \xi_S^{-2})(v'_S \xi_L^{-2} + v'^{-1}_L \alpha'_{ratio})\right], \end{aligned} \tag{A.5}$$

for which the quantities $\xi_L = (v'^{-2}_{Ray} - v'^{-2}_L)^{-1/2}$ and $\xi_S = (v'^{-2}_{Ray} - v'^{-2}_S)^{-1/2}$ have been introduced for the sake of convenience.

References

[1] Kanai K 1950 "The effect of solid viscosity of surface layer on the earthquake movements" *Bulletin of the Earthquake Research Institute, Tokyo University, Tokyo, Japan* **28** pp 31–35

[2] Aki K and Richards P G 1980 *Quantitative Seismology: Theory and Methods* (San Francisco, CA, USA: W. H. Freeman and Company)

[3] Gao L, Parker K J, Lerner R M, and Levinson S F 1996 "Imaging of the elastic properties of tissue: A review" *Ultrasound in Medicine & Biology* **22**(8) pp 959–977

[4] Rollins F R Jr 1966 "Critical ultrasonic reflectivity: A tool for material evaluation" *Materials Evaluation* **24**(12) pp 683–689

[5] Fitch C E Jr and Richardson R L 1967 "Ultrasonic wave models for nondestructive testing interfaces with attenuation" in *Progress in Applied Materials Research **8** (London, England: Iliffe Books, eds. Stanford E G, Fearon J H, and McGounagle W J)* pp 79–120

[6] Trivett D, Luker L, Petrie S, Van Buren A, and Blue J 1990 "A planar array for the generation of evanescent waves" *The Journal of the Acoustical Society of America* **87**(6) pp 2535–2540

[7] Itou H, Furuya K, and Haneda Y 2011 "Evanescent wave reproduction using linear array of loudspeakers" *Proceedings of the IEEE Workshop on Applications of Signal Processing to Audio and Acoustics, New Paltz, NY, USA* pp 37–40

[8] Shaw R P and Bugl P 1969 "Transmission of plane waves through layered linear viscoelastic media" *The Journal of the Acoustical Society of America* **46**(3B) pp 649–654

[9] Matula T J and Marston P L 1993 "Electromagnetic acoustic wave transducer for the generation of acoustic evanescent waves on membranes and optical and capacitor wave-number selective detectors" *The Journal of the Acoustical Society of America* **93**(4) pp 2221–2227

[10] Deschamps M 1994 "Reflection and refraction of the evanescent plane wave on plane interfaces" *The Journal of the Acoustical Society of America* **96**(5) pp 2841–2848

[11] Borcherdt R D 2009 *Viscoelastic Waves in Layered Media* (Cambridge, England: Cambridge University Press)

[12] Brinson H F and Brinson L C 2008 *Polymer Engineering Science and Viscoelasticity: An Introduction.* (New York, NY, USA: Springer)

[13] Jones D G 2001 *Handbook of Viscoelastic Vibration Damping* (West Sussex, England: Wiley)

[14] Borcherdt R D 1973 "Energy and plane waves in linear viscoelastic media" *Journal of Geophysical Research* **78**(14) pp 2442–2453

[15] Borcherdt R D and Wennerberg L 1985 "General P, type-I S, and type-II S waves in anelastic solids: Inhomogeneous wave fields in low-loss solids" *Bulletin of the Seismological Society of America* **75**(6) pp 1729–1763

[16] Buchen P W 1971 “Plane waves in linear viscoelastic media” *Geophysical Journal International* **23**(5) pp 531–542
[17] Wennerberg L and Glassmoyer G 1986 “Absorption effects on plane waves in layered media” *Bulletin of the Seismological Society of America* **76**(5) pp 1407–1432
[18] Lockett F J 1962 “The reflection and refraction of waves at an interface between viscoelastic materials” *Journal of the Mechanics and Physics of Solids* **10**(1) pp 53–64
[19] Cooper H F Jr and Reiss E L 1966 “Reflection of plane viscoelastic waves from plane boundaries” *The Journal of the Acoustical Society of America* **39**(6) pp 1133–1138
[20] Cooper H F Jr 1967 “Reflection and transmission of oblique plane waves at a plane interface between viscoelastic media” *The Journal of the Acoustical Society of America* **42**(5) pp 1064–1069
[21] Schoenberg M 1971 “Transmission and reflection of plane waves at an elastic–viscoelastic interface” *Geophysical Journal International* **25**(1–3) pp 35–47
[22] Borcherdt R D 1982 “Reflection–refraction of general P-and type-I S-waves in elastic and anelastic solids” *Geophysical Journal International* **70**(3) pp 621–638
[23] Bertoni H L and Tamir T 1973 “Unified theory of Rayleigh-angle phenomena for acoustic beams at liquid-solid interfaces” *Applied Physics* **2**(4) pp 157–172
[24] Norris A N 1983 “Back reflection of ultrasonic waves from a liquid–solid interface” *The Journal of the Acoustical Society of America* **73**(2) pp 427–434
[25] Woods D C, Bolton J S, and Rhoads J F 2015 “On the use of evanescent plane waves for low-frequency energy transmission across material interfaces” *The Journal of the Acoustical Society of America* **138**(4) pp 2062–2078
[26] Becker F L and Richardson R L 1969 “Critical-angle reflectivity” *The Journal of the Acoustical Society of America* **45**(3) pp 793–794
[27] Becker F L and Richardson R L 1972 “Influence of material properties on Rayleigh critical-angle reflectivity” *The Journal of the Acoustical Society of America* **51**(5B) pp 1609–1617
[28] Szabo T L and Wu J 2000 “ A model for longitudinal and shear wave propagation in viscoelastic media” *The Journal of the Acoustical Society of America* **107**(5) pp 2437–2446
[29] Brekhovskikh L M 1960 *Waves in Layered Media* (New York, NY, USA: Academic Press)
[30] Beyer R T and Letcher S V 1969 *Physical Ultrasonics* (New York, NY, USA: Academic Press)
[31] Cheeke J D N 2012 *Fundamentals and Applications of Ultrasonic Waves.* (Boca Raton, FL, USA: CRC Press)
[32] Breazeale M A, Adler L, and Flax L 1974 “Reflection of a Gaussian ultrasonic beam from a liquid–solid interface” *The Journal of the Acoustical Society of America* **56**(3) pp 866–872
[33] Plona T J, Pitts L E, and Mayer W G 1976 “Ultrasonic bounded beam reflection and transmission effects at a liquid/solid-plate/liquid interface” *The Journal of the Acoustical Society of America* **59**(6) pp 1324–1328
[34] Claeys J M and Leroy O 1982 “Reflection and transmission of bounded sound beams on half-spaces and through plates” *The Journal of the Acoustical Society of America* **72**(2) pp 585–590
[35] Van Den Abeele K and Leroy O 1993 “Complex harmonic wave scattering as the framework for investigation of bounded beam reflection and transmission at plane interfaces and its importance in the study of vibrational modes” *The Journal of the Acoustical Society of America* **93**(1) pp 308–323